

# INFLUENCE OF RARE-EARTH DOPING ON THE ELECTRICAL PROPERTIES OF HIGH VOLTAGE GRADIENT ZnO VARISTORS

#LEI KE\*, YANHONG YUAN\*, HUA ZHAO\*, XUEMING MA\*\*

\*Institute of Applied Mathematics and Physics, Shanghai Dianji University, Shanghai 201306, P. R. China

\*\*State Key Laboratory of Precision Spectroscopy, Department of Physics,  
East China Normal University, Shanghai 200241, P. R. China

#E-mail: kelei.sdju@gmail.com

Submitted March 3, 2012; accepted April 21, 2013

**Keywords:** ZnO varistors, Rare-earth doping, Voltage gradient, Electrical properties

*The influence of rare-earth doping on the electrical properties of ZnO varistors was investigated. In a lower doping region, the electrical properties were greatly improved with the increase of rare-earth contents. The highest voltage gradient value of 1968.0 V/mm was obtained with a rare-earth concentration of 0.06 mol. %. The microstructure of samples with different amounts of rare-earth oxides was examined and the notable decrease of grain size was identified as the origin for the increased voltage gradient. The doped rare-earth oxides dissolved at the grain boundaries and the excessive doping reduced the voltage across the single grain/grain boundary from 2.72 V to 0.91 V. The poor electrical properties in a higher doping region resulted from the degeneration of grain boundaries and the decrease of block density.*

## INTRODUCTION

ZnO varistors are polycrystalline multicomponent ceramics produced by sintering ZnO together with other minor additives, such as Bi<sub>2</sub>O<sub>3</sub>, Sb<sub>2</sub>O<sub>3</sub>, Co<sub>2</sub>O<sub>3</sub>, Cr<sub>2</sub>O<sub>3</sub>, MnO<sub>2</sub>, etc. They are ceramic semiconductor devices that exhibit highly nonlinear current-voltage ( $I$ - $V$ ) characteristics enabling them to be efficient overvoltage protectors in the equipment for power transmission [1, 2]. Microstructurally, the excellent nonlinear properties are attributed to the electrostatic potential barrier at the grain boundaries containing many interface states. The semiconducting n-type ZnO grains and the thin insulating intergranular layers surrounding them can be considered as structural units that correspond to micro-varistors [3, 4]. The nonlinear  $I$ - $V$  relationship is expressed by the empirical equation  $J = KE^\alpha$ , where  $J$  is the current density,  $E$  is the voltage gradient,  $K$  is a constant that depends on the microstructure and the exponent  $\alpha$  is the nonlinearity exponent [5, 6]. The nonlinear region of some ZnO materials extends over several orders of magnitude in current. This extensive non-ohmic behavior together with an ability to repeatedly withstand relatively high power pulses has resulted in their widespread application as voltage surge protectors in electrical circuits [7, 8].

Most of previously reported ZnO varistors have based on the original composition invented by Matsuoka in 1969 [1] and exhibit excellent varistor properties. However, the requirement of high voltage gradient is becoming more important with the increasing use of

ZnO varistors as surge-suppressing elements [9]. It is well known that a reduction in grain size is the key for enhancing the voltage gradient of ZnO varistors [10]. At present time, some techniques of manufacturing ZnO varistors with high voltage gradient have been reported on many occasions. Several new additives (mainly other metal oxides) have been added in order to modify the varistor properties. Some of them substitute for zinc atoms in the lattice whereas others, such as trivalent rare-earth ions, which act as grain growth inhibitors, remain mainly localized as aggregates at the grain boundaries or in the intergranular layers [11, 12].

The rare-earth dopants have an effect on the low-current region of varistors and determine the breakdown voltage [8]. It is found that the rare-earth doping could significantly improve the voltage gradient, as well as the leakage current and the nonlinearity exponent. The purpose of present paper is to investigate the influence of rare-earth doping on the microstructure development and the electrical properties of ZnO varistors.

## EXPERIMENTAL

Varistor samples were fabricated by the conventional ceramic fabrication procedure. Appropriate amounts of raw chemicals were weighed with the composition of (96.5-3X) mol.% ZnO + 0.7 mol.% Bi<sub>2</sub>O<sub>3</sub> + 1.0 mol.% Sb<sub>2</sub>O<sub>3</sub> + 0.5 mol.% Cr<sub>2</sub>O<sub>3</sub> + 0.8 mol.% Co<sub>2</sub>O<sub>3</sub> + 0.5 mol.% MnO<sub>2</sub> + X mol.% (Y<sub>2</sub>O<sub>3</sub> + Dy<sub>2</sub>O<sub>3</sub> + Er<sub>2</sub>O<sub>3</sub>), where X = = 0.00, 0.01, 0.02, 0.03, 0.04, 0.05, 0.06, 0.07, 0.08,

0.09 and 0.10 (samples labeled as RE0, RE1, RE2, RE3, RE4, RE5, RE6, RE7, RE8, RE9 and RE10, respectively). The mixed powders were homogenized in absolute ethanol using a high-energy planetary mill with stainless steel balls in a nylon bottle for 5 h and then dried at 120°C for 2 h. An organic binder addition of 2 wt. % polyvinyl alcohol (PVA) was added to the milled powders to favour pressing of the compacts (the organic was slowly burnt out at about 500°C). Green cylindrical compacts were uniaxially pressed at 800 MPa into discs with a diameter of 10 mm and a thickness of 1 mm. The pellets were calcined at 800°C for 2 h and cooled to room temperature freely, whereas the heating rate to the sintering temperature was typically 4°C/min. Disc type specimens were used for electrical measurements and Ag-paste was applied as a conducting electrode on the sintered body. The electrodes were formed by heating at 600°C for 15 minutes on both faces of the pellets and 8 mm in diameter.

The electrical properties of varistors were measured using a DC parameter instrument (DC-PI, CJ1001). The breakdown voltage ( $U_{ImA}$ ) was measured at the current density of 1.0 mA/cm<sup>2</sup> and the voltage gradient ( $E_{ImA}$ ) was obtained by  $E_{ImA} = U_{ImA}/D$ , where  $D$  is the thickness of sample. The leakage current ( $I_L$ ) was measured at the electrical field of 0.75  $U_{ImA}$  and the nonlinearity exponent ( $\alpha$ ) was determined in the current density range of 1.0 mA/cm<sup>2</sup> to 10 mA/cm<sup>2</sup>, according to the expression of  $\alpha = 1/(\log E_{10mA} - \log E_{1mA})$ . The bulk density ( $\rho$ ) measurements of sintered ceramics were carried out by Archimedes method and the relative theoretical density values ( $\rho_{rt}$ ) were determined by using the equation of  $\rho_{rt} = \rho/\rho_t$ , where  $\rho_t = 5.65$  g/cm<sup>3</sup>, is the theoretical density of ZnO. The crystalline phase composition on the pellets of sintered ceramics was identified by an X-ray diffractometry (XRD, D/max 2550V) using CuK $\alpha$  radiation. Microstructure characterization of varistors was conducted by scanning electron microscopy (SEM, JSM-5610LV) after etching for a few seconds in 1 wt. % hydrochloric acid ethanol solution. The average grain

sizes ( $d$ ) were determined by the linear intercept method from the SEM micrographs, measuring between 30 and 50 grains. A stereological correction factor of 1.56 was used to convert from average intercept distance to grain diameter [13]. The voltage values across the single grain/grain boundary ( $U_g$ ) were calculated from the equation of  $U_g = E_{ImA} d/1000$ . The composition of the grain boundary region was determined by an energy dispersive X-ray spectroscopy (EDXS, Inca) system attached to the SEM. The detailed parameters, including barrier height ( $\phi_B$ ), depletion layer width ( $\omega$ ), donor concentration ( $N_D$ ) and density of interface states ( $N_S$ ), were calculated by capacitance-voltage ( $C-V$ ) measurement at 1 kHz as test frequency using a precision LCR analyzer (HP4284A).  $\phi_B$  and  $N_D$  were determined by the equation  $(1/C_B - 1/C_0)^2 = 2(\phi_B + U_{gb})/e\epsilon N_D$  [14], where  $C_B$  is the capacitance per unit area of a grain boundary,  $C_0$  is the value of  $C_B$  when  $U_{gb} = 0$ ,  $U_{gb}$  is the applied voltage per grain boundary,  $e$  is the charge of a single electron,  $\epsilon$  is the permittivity of ZnO ( $\epsilon = 8.5\epsilon_0$ ). The DC aging test was performed for the stress state of 0.75  $E_{ImA}/120^\circ\text{C}$ . Simultaneously,  $I_L$  was monitored at the intervals of 30 minutes during stressing using a 4(1/2) digit bench-type digital multimeter.

## RESULTS AND DISCUSSION

Figure 1 shows the electrical parameters of ZnO varistors including  $E_{ImA}$ ,  $I_L$  and  $\alpha$ , as a function of rare-earth doping concentration. As can be seen in Figure 1a), the  $E_{ImA}$  values are significantly affected after rare-earth doping. With the increase of rare-earth content,  $E_{ImA}$  increases at first and then decreases. The  $E_{ImA}$  value for sample RE0 without any rare-earth oxides is only 1648.9 V/mm, but it achieves the maximum value of 1968.0 V/mm for sample RE2 with the total doping concentration of 0.06 mol. %. Samples with better electrical parameters are obtained in the doping concentration range between 0.06~0.09 mol. %, of which the  $E_{ImA}$  values are increased by 18.4~19.4 %.

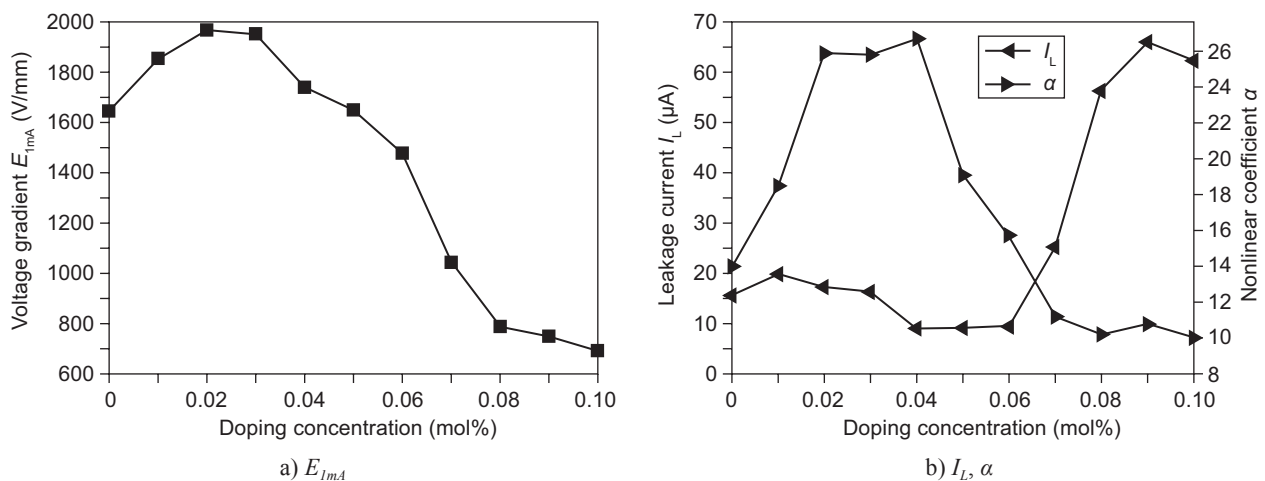


Figure 1. Electrical parameters as a function of rare-earth doping concentration for ZnO varistor.

An excessive rare-earth doping concentration greatly decreases the  $E_{1mA}$  value. It decreases to below 1000 V/mm in  $E_{1mA}$  when  $Y_2O_3$ ,  $Dy_2O_3$  and  $Er_2O_3$  are all over 0.08 mol. % (samples RE8, RE9 and RE10). Figure 1b shows the variation of  $I_L$  and  $\alpha$  with different amounts of rare-earth oxides. On the whole, the variation of  $I_L$  is opposite to that of  $\alpha$ . The measured values of  $I_L$  and  $\alpha$  for the sample without any rare-earth oxides are 15.62  $\mu A$  and 14.0. The effects on  $I_L$  and  $\alpha$  with different doping concentration are similar to that on  $E_{1mA}$ . Doped samples with better  $I_L$  and  $\alpha$  are obtained in the lower doping concentration region, approximately between 0.06 and 0.12 mol. % (samples RE2, RE3 and RE4). Once beyond this range,  $I_L$  increases steeply and  $\alpha$  decreases abruptly, which indicates that the electrical properties of samples are deteriorated. To easily find the rare-earth doping effect on the electrical properties of ZnO varistors, samples RE0, RE2 and RE10 are selected for a detailed comparison on  $I$ - $V$  characteristics. Sample RE0 represents the undoped sample, while samples RE2 and RE10 represent the rare-earth doped samples with the optimum/excessive doping concentration, respectively. Figure 2 shows the current density-voltage gradient ( $J$ - $E$ ) curves for the selected three samples with different rare-earth doping concentration. The undoped sample RE0 shows a relatively low value of the voltage gradient. On adding 0.06 mol. % rare-earth content in sample RE2, the voltage gradient is significantly enhanced. However, a much higher dopant concentration, such as 0.30 mol. % for sample RE10, leads to worse electrical properties. Therefore, the electrical properties of ZnO varistors

are greatly improved with small amounts of rare-earth dopants, but severely deteriorated when excessive amounts of rare-earth dopants are added. In our experiments, the optimum doping concentration range is between 0.06~0.09 mol. %, and the 0.06 mol. %-doped sample RE2 has the highest value of voltage gradient.

The XRD patterns of ZnO varistors are shown in Figure 3. These patterns reveal the presence of  $Zn_7Sb_2O_{12}$  and  $Bi_2O_3$  peaks as the minor secondary phases, in addition to the primary phase of ZnO. The revealed phases are identical to those in the  $Bi_2O_3$ -based ZnO varistors. However, one can also observe the presence of rare-earth phase for doped samples RE2 and RE10. In Figure 3b) and c), two diffraction peaks appear obviously in the range of 48~51°. As we know, the characteristic diffraction angle of rare-earth oxides is between 48° and 51°. For example, the diffraction angle of  $Y_2O_3$  is 48.791°/50.395° (PDF 74-1828), the diffraction angle of  $Er_2O_3$  is 48.860°/50.467° (PDF 77-0777). Therefore, the appearance of two diffraction peaks in the range of 48~51° can be seen as the superposition of all the rare-earth oxides. The ionic radius of rare-earth element ( $Y^{3+}$ : 0.089 nm,  $Dy^{3+}$ : 0.091 nm,  $Er^{3+}$ : 0.088 nm) is larger than  $Zn^{2+}$  (0.074 nm). The great difference of ionic radii and electrocharge numbers between rare-earth ions and zinc ions makes it difficult for the rare-earth ions to solid dissolve into ZnO grains at the sintering temperature of 800°C. The rare-earth ions dissolve at the grain boundaries and exist in the forms of  $Y_2O_3$ ,  $Dy_2O_3$  and  $Er_2O_3$ , which has been verified by EDXS analysis. Figure 4 shows the EDXS microanalysis of grain boundary

Table 1. Electrical and microstructural parameters of ZnO varistors with different amounts of rare-earth oxides.

Sample	$E_{1mA}$ (V/mm)	$I_L$ ( $\mu A$ )	$\alpha$	$\rho_{rt}$ (%)	$d$ ( $\mu m$ )	$U_g$ (V)	$\phi_B$ (eV)	$\omega$ (nm)	$N_D$ ( $\times 10^{18}/cm^3$ )	$N_S$ ( $\times 10^{12}/cm^2$ )
RE0	1648.9	15.62	14.0	97.25	1.60	2.64	0.85	17	2.9	4.8
RE2	1968.0	17.33	25.9	97.17	1.38	2.72	0.87	13	5.1	6.5
RE10	700.2	62.38	10.0	93.98	1.29	0.91	0.75	40	0.5	1.8

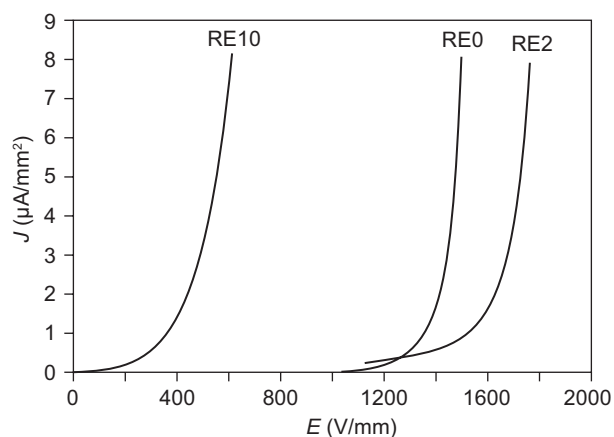


Figure 2.  $J$ - $E$  curves for the samples with different amounts of rare-earth oxides.

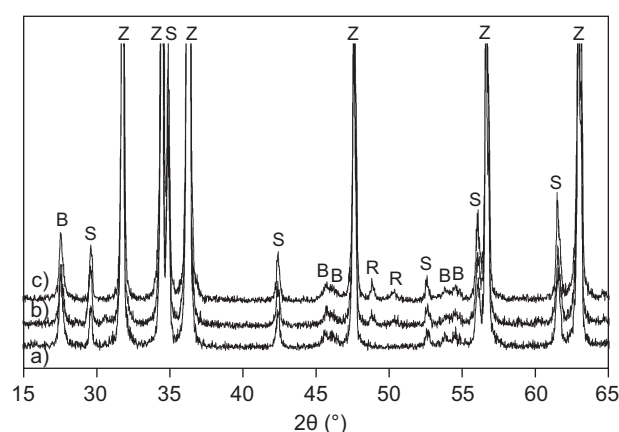


Figure 3. XRD data of the selected three samples - a) RE0, b) RE2 and c) RE10.



region for the undoped sample RE0 and doped sample RE2. Compared with sample RE0, there appears a new EDXS peak at 1.5 keV for the sample RE2. This new peak can be attributed to the doping of rare-earth oxides. The dissolved rare-earth ions have no effect on the lattice structure of ZnO. They form small particles along the edges of the ZnO grains and as a result pin the grains, restricting their growth. The decrease of the grain size implies an increase in the amount of grain boundaries, and thus also in  $E_{ImA}$ . SEM micrographs of ZnO varistors doped with different amounts of rare-earth oxides are shown in Figure 5. It is observed that as the rare-earth content rises, the number of crystals located at the grain boundaries increases, leading to a size reduction of ZnO grains from 1.60 to 1.29  $\mu\text{m}$ , as listed in Table 1. Initially, the improvement of  $E_{ImA}$  is attributed to the increase in the number of grain boundaries caused by the decrease of ZnO grain size. Then, the change of grain size is small with the further addition, which saturated at  $\sim 1.2 \mu\text{m}$ , and the abrupt decrease of  $E_{ImA}$  is attributed to a degeneration in the quality of grain boundaries. Sample RE10 doped with excessive amounts of rare-earth oxides exhibits much lower  $U_g$  than the general value of 2–3 V [15]. Although the excessively doped sample RE10 has a fine grain size, it exhibits very poor electrical properties due to its bad grain boundaries.

Detailed microstructural parameters are summarized in Table 1. The calculated results indicate that sample RE2 has the maximum value of barrier height  $\phi_B$  and the minimum value of depletion layer width  $\omega$ . The variations of  $\phi_B$  and  $\omega$  result from the Schottky barrier at the grain boundary. A high and narrow Schottky barrier is helpful to improve the electrical properties of ZnO varistors, especially in  $E_{ImA}$  and  $\alpha$ . By doping 0.06 mol. % rare-earth oxides, the values of  $U_g$  and  $\phi_B$  are increased by 3.0 % and 2.4 %, respectively. Higher doping causes them to decrease down to 0.91 V and 0.75 eV when the rare-earth amounts are 0.30 mol. %. This coincides to the variation of  $E_{ImA}$  and  $\alpha$  in the  $I$ - $V$  characteristics. The value of donor concentration  $N_D$  increases in the range of  $2.9\sim 5.1\times 10^{18}/\text{cm}^3$

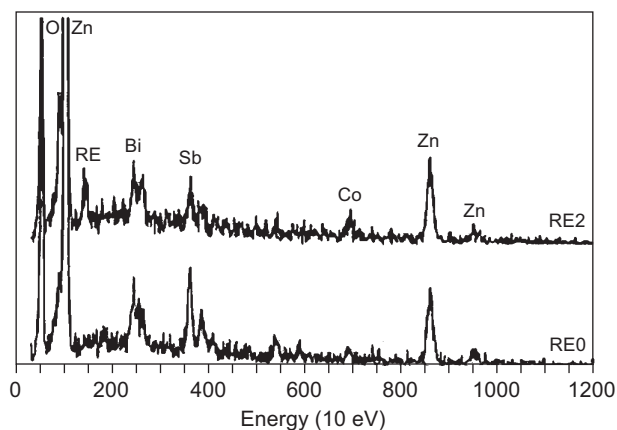
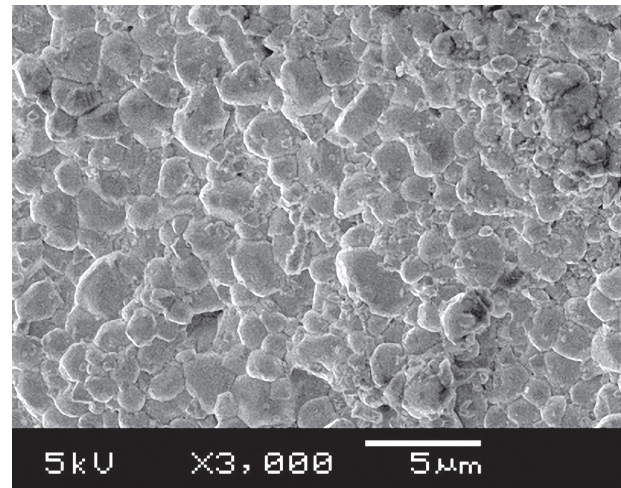
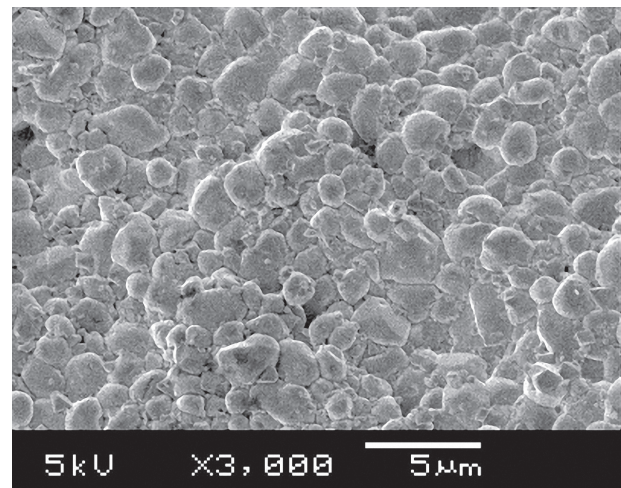


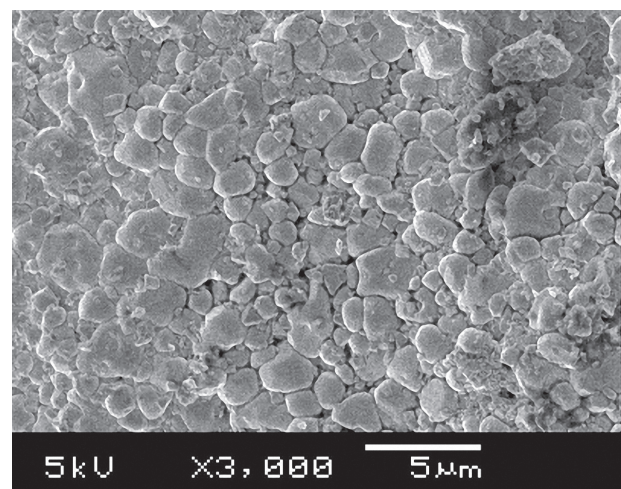
Figure 4. EDXS spectra recorded across the grain boundary region for the samples RE0 and RE2.



a) RE0



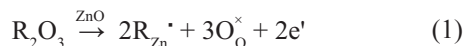
b) RE2



c) RE10

Figure 5. SEM micrographs of the selected three samples - a) RE0, b) RE2 and c) RE10.

with increasing rare-earth contents, which means the rare-earth oxides act as donors. Although the rare-earth ions have larger radii than  $Zn^{2+}$ , a limited substitution within the ZnO grains is possible. The rare-earth ions substitute for  $Zn^{2+}$  and create lattice defects in ZnO grains. The chemical-defect reaction can be written:



where  $R_{Zn}^{\bullet}$  is a positively charged rare-earth ion substituted for Zn lattice site and  $O_O^{\times}$  is a neutral oxygen of oxygen lattice site. The electron generated in the reaction above increases the donor concentration. On the other hand, when the excessive rare-earth oxides exist over the solubility limit in the system, they will aggregate at the grain boundaries. As a result, the grain boundary structure is destroyed and the amount of pores increases, which directly result in the significant decrease in the  $U_g$  and  $\rho_{rt}$  values of sample RE10.

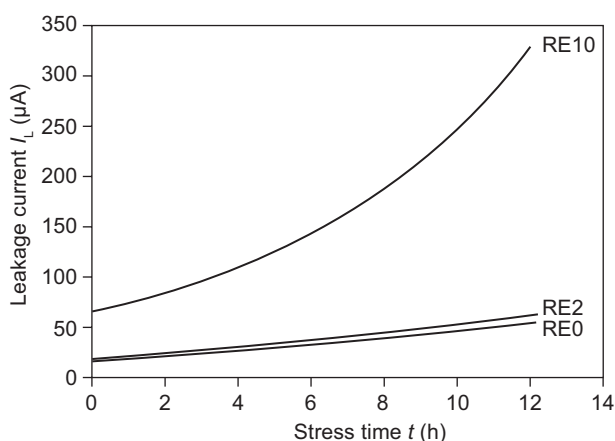


Figure 6. DC aging behavior of the samples with different amounts of rare-earth oxides.

ZnO varistors begin to degrade because of gradually increasing  $I_L$  with stress time. The electrical stability is a technologically important characteristic of varistors. Figure 6 shows the DC aging behavior of three samples with different rare-earth doping concentrations during the stress of  $0.75 E_{1mA}/120^\circ C$ . All the  $I_L$  values increase with increasing stress time, which indicates that the varistors are degraded under the DC bias. Compared with sample RE2, sample RE10 has a large variation in  $I_L$  during the DC stress. In light of the results, it can be concluded that the resistance against DC aging stress is greatly affected by the rare-earth doping. A higher doping concentration of 0.30 mol. % directly makes the electrical stability become worse. After being stressed for 12 h, the  $I_L$  value of sample RE10 increases to more than 300  $\mu A$ . But the  $I_L$  value of sample RE2 increases only from 17.33 to 57.50  $\mu A$ . The small change in  $I_L$  for sample RE2 shows that an appropriate doping proportion of rare-earth oxides has no obviously deteriorating effect on ZnO varistors.

## CONCLUSIONS

The electrical properties of ZnO varistors are affected by doping rare-earth oxides. The  $E_{1mA}$  values of doped samples increase at first and then decrease with the increase of rare-earth content. The highest  $E_{1mA}$  value 1968.0 V/mm is obtained with the rare-earth amounts of 0.06 mol. %. The rare-earth dopants can also greatly improve  $I_L$  and  $\alpha$ . Doped ZnO varistors with better  $I_L$  and  $\alpha$  are obtained in the doping region below 0.12 mol. %. In this doping region, the increase of  $E_{1mA}$  results from the decrease in average grain size. The sample doped 0.06 mol. % rare-earth content has an average grain size of 1.38  $\mu m$ , a barrier height of 0.87 eV, a depletion layer width of 13 nm, a donor concentration of  $5.1 \times 10^{18}/cm^3$  and a interface state density of  $6.5 \times 10^{12}/cm^2$ . Small grain size and good grain boundary barrier are helpful to increase the single grain/grain boundary voltage and improve the electrical stability of ZnO varistors. But excessive amounts of rare-earth dopants tend to aggregate at the grain boundaries and destroy the grain boundary structure, which will finally deteriorate the electrical properties of ZnO varistors.

## Acknowledgement

The authors gratefully acknowledge the financial support of the National Natural Science Foundation of China (Grant No. 10804071), Shanghai Municipal Education Commission Project (Grant No. 12AZ16 and No. 12YZ185) and Shanghai Dianji University Project (Grant No. 11C409 and No. 12XKJC01).

## REFERENCES

1. Matsuoka M., Masuyama T., Iida Y.: Jpn. J. Appl. Phys. 8, 1275 (1969).
2. Matsuoka M.: Jpn. J. Appl. Phys. 10, 736 (1971).
3. Eda K.: J. Appl. Phys. 49, 2964 (1978).
4. Gupta T. K., Carlson W. G.: J. Mater. Sci. 20, 3487 (1985).
5. Gupta T. K.: J. Am. Ceram. Soc. 73, 1817 (1990).
6. Clark D. R.: J. Am. Ceram. Soc. 82, 485 (1999).
7. Levinson L. M., Philipp H. R.: Am. Ceram. Soc. Bull. 65, 639 (1986).
8. Shichimiya S., Yamaguchi M., Furuse N., Kobayashi M., Ishibe S.: IEEE Trans. Power Delivery 13, 465 (1998).
9. Nan C. W., Clarke D. R.: J. Am. Ceram. Soc. 79, 3185 (1996).
10. Peiteado M., Fernandez J. F., Caballero A. C.: J. Eur. Ceram. Soc. 25, 2999 (2005).
11. Bernik S., Macek S., Bui A.: J. Eur. Ceram. Soc. 24, 1195 (2004).
12. Bernik S., Daneu N.: J. Eur. Ceram. Soc. 27, 3161 (2007).
13. Wurst J. C., Nelson J. A.: J. Am. Ceram. Soc. 55, 109 (1972).
14. Mukae K., Tsuda K., Nagasawa I.: J. Appl. Phys. 50, 4475 (1979).
15. Mahan G. D., Levinson L. M., Philipp H. R.: J. Appl. Phys. 50, 2799 (1979).